Supplementary Information

DNP Signal Enhancement with High-Affinity Biradical Tags

Rivkah Rogawski, Ivan V. Sergeyev, Yongjun Li, M. Francesca Ottaviani, Virginia Cornish, Ann E. McDermott

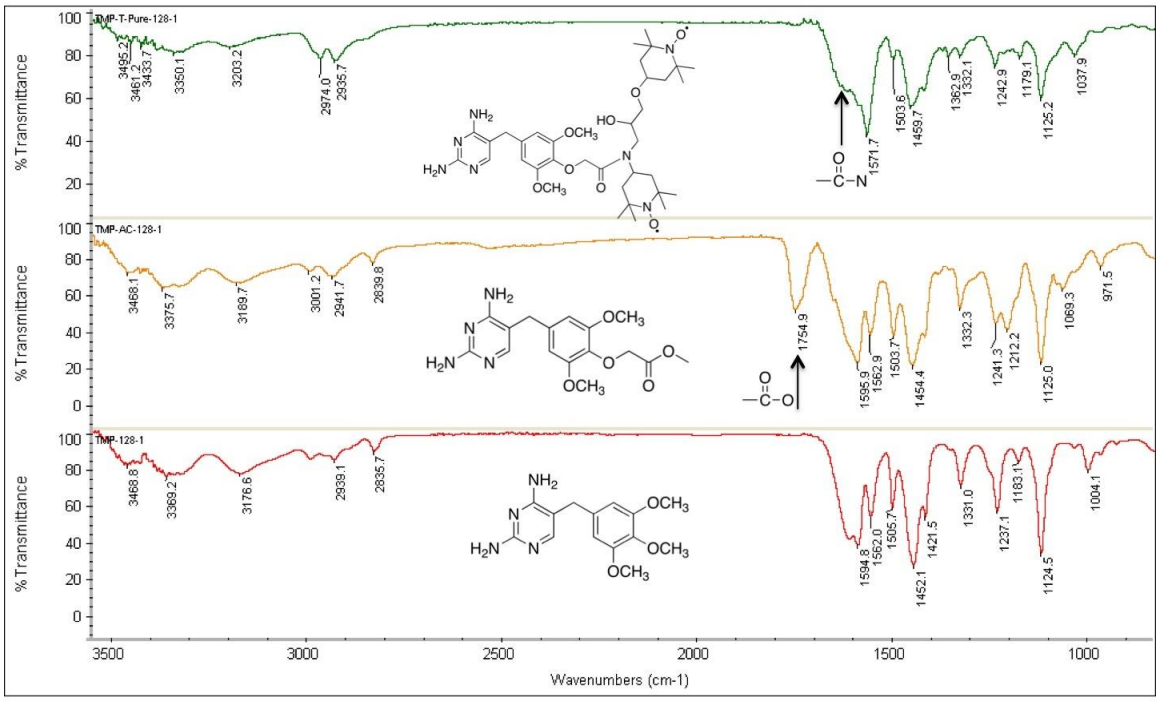

Figure S1: ATR-FTIR spectrum of TMP-T (top, green), with TMP-ester (middle, orange) and TMP (bottom, red) for comparison purposes**.**

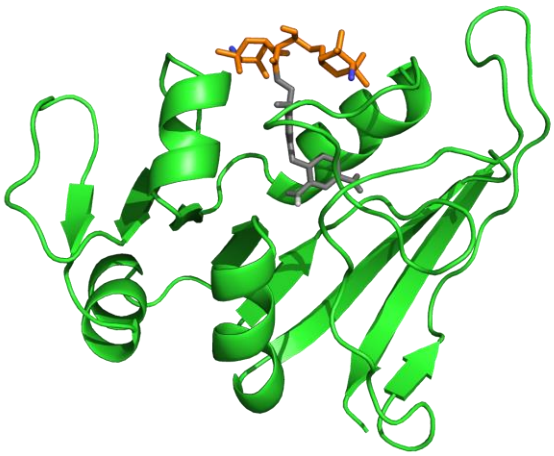

Figure S2: DHFR (green, PDB accession code 1RX1[13]) bound to TMP-T (TMP moiety-gray, TOTAPOL moiety- orange) made by docking TMP-T using Autodock Vina[14].

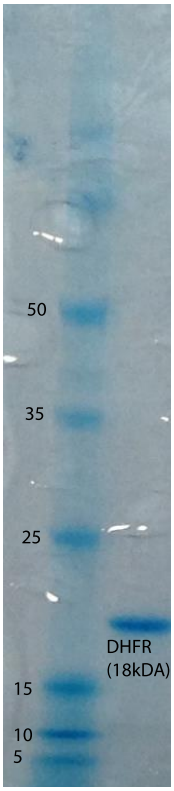

Figure S3: Gel of purified DHFR used in all experiments shows that protein is pure, with a band appearing at ~18 kDa, the molecular weight of DHFR.

TMP-T:

Concentration/Components			ε (protein)	T_B (s) (protein)	^1H T_1, CP-detected (s)
[DHFR]	[TMP-T]	Other			
8.0 mM	-		N/A	N/A	4.1±0.1*
4.9 mM	2.7 mM	4 mM glucose	13.5 ± 0.5	5.2±0.2	3.8±0.2
4.5 mM	4.5 mM	3 mM ^{13}C-glucose	22.5 ± 0.5**	4.1 ±0.2	2.8±0.2
3.0 mM	7.0 mM		26 ± 1**	N/A	1.9±0.4*
0.5 mM	0.5 mM	>98% ^{2}H	19 ± 2 **	4.1 ± 0.4	2.2 ± 0.2
0.05 mM	0.05 mM	>98% ^{2}H	15 ±2**	3.3±0.5	N/A
4.2 mM	2.3 mM	3 mM glucose 22 mM TMP 15% v/v DMSO	6.9 ± 0.1	12.6±0.2	3.6±0.2
0.5 mM	0.5 mM	20% ^{1}H	8 ± 1	32 ±4	N/A

TOTAPOL:

Concentration/Components			ε (protein)	T_B (s)	^1H T_1, CP-detected (s)
[DHFR]	[TOTAPOL]	Other			
7.5 mM	4 mM		17.8 ± 0.5**	5.1±0.2	3.7±0.3
5 mM	10 mM		22.5 ± 0.5**	3.3±0.1	2.5±0.1
6.5 mM	20 mM		28 ± 2 **	2.3±0.1	1.9±0.1
0.5 mM	1 mM		5.0 ± 0.5**	27±8	N/A
0.05 mM	0.1 mM		1.5 ± 0.5**	N/A	N/A
0.5 mM	21 mM	>98% ^{2}H	28 ± 3	4.1±0.1	N/A
0.5 mM	21 mM	20% ^{1}H	27 ± 1	3.5±0.1	N/A

*Data were collected using a different probe and should not be compared directly to all other values in this table. The two probes exhibited differing ^{1}H field homogeneities.
**Data used in Figure 2

Table S1: Sample composition and observed DNP enhancement, DNP buildup time, and ^{1}H T_1 for samples prepared with TMP-T and TOTAPOL (for comparative purposes). For samples with low S/N, ^{1}H T_1 and/or T_B could not be measured.

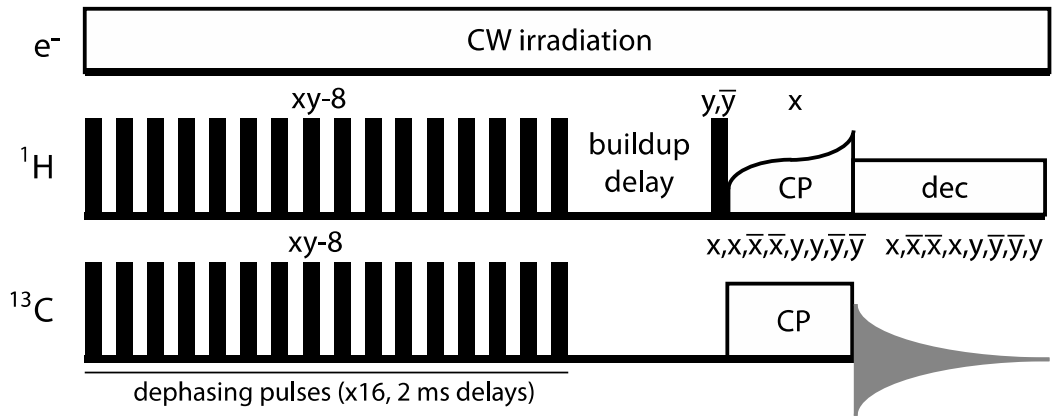

Figure S4: Pulse sequence used for DNP buildup time measurements[1], with phase cycles noted above each element. Under continuous wave microwave irradiation of the electrons, a train of 16 π/2 pulses (2.5 μs and 4.0 μs for ^{1}H and ^{13}C, respectively), separated by 2 ms each, is used to destroy any ^{1}H and ^{13}C polarization prior to a variable buildup delay, which is incremented exponentially in 16 steps from 0.1 μs to 64 s. After allowing ^{1}H polarization build up via DNP enhancement during the buildup delay, a ^{1}H π/2 pulse (2.5 μs) and a ^{1}H-^{13}C cross-polarization (CP) element are used to transfer polarization to ^{13}C for detection. 100 kHz SPINAL-64[2] ^{1}H decoupling is applied during acquisition. Buildup values are extracted from the data by fitting peak integrals as a function buildup time to a saturation recovery function of the form $I(t) = I(0) * (1 - \exp(-t/T_B))$.

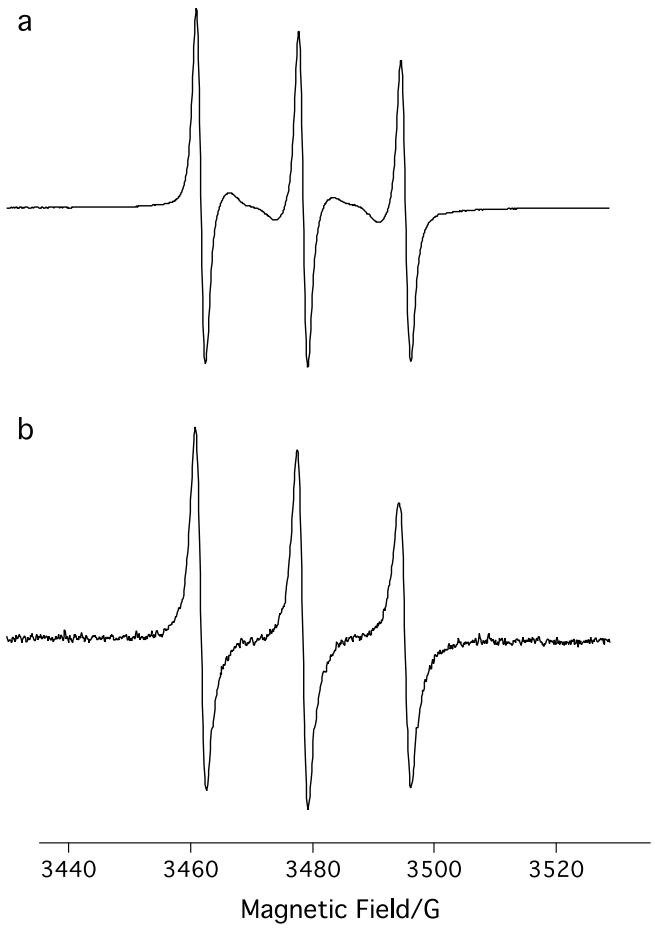

Figure S5: Room temperature CW 9.5 GHz EPR spectra of a) 0.1 mM TOTAPOL and b) 0.1 mM TMP-T. The EPR spectrum of TOTAPOL shows a dominant three-line ^{14}N hyperfine splitting (such as is seen for monomeric TEMPO), along with two additional features that have been attributed to inter-nitroxide spin-spin exchange coupling J[3]. The details of the spectra are known to be affected by solvent interactions and molecular environment[4,5]. The spectrum of TMP-T is broadened relative to that of TOTAPOL and shows decreased electron exchange. This is likely due to derivatization, which may lead to reduced mobility, polarity, and transient intramolecular interactions with the hydrophobic trimethoprim moiety.

Fluorescence polarization binding experiments

TMP-TAMRA, a fluorescent-tagged trimethoprim analog, was prepared by Dr. Zhixing Chen of the Cornish group according to published procedure [6] (see Figure S6) and characterized by Dr. Yao Zong Ng, also of the Cornish group. For fluorescence polarization experiments, 0.5 μM DHFR in PBS was incubated with 0.25 μM TMP-TAMRA and TMP-T concentrations ranging from 1 nM to 100 uM. Fluorescence anisotropy was measured in 96 well black-bottom plates on a Victor X5 microplate reader, using an excitation wavelength of 530 nm and an emission wavelength of 595 nm. Fluorescence anisotropy of control samples without protein was measured to ensure that anisotropy reached its minimum value. Anisotropy as a function of TMP-T concentration was plotted on a semi-log plot and fit in IgorPro with a sigmoidal binding equation to obtain an IC_{50} of 2.8 ± 0.1 uM with a χ^2 value of 2.94279e-05 (see Figure S7).

This IC_{50} was converted to a K_d of 165 ± 7 nM using the following equation[7] :

$K_{d,I} = [I]_{50} / ([L]_{50}/K_d + [P]_0/K_d + 1)$

A K_d value for TMP-TAMRA of 30 nM, and with all relevant parameters calculated as in Kenakin et al.[8] The K_d of TMP-TAMRA was calculated in a separate competition experiment with the native ligand, trimethoprim, using the published binary K_d of 15 nM[9].

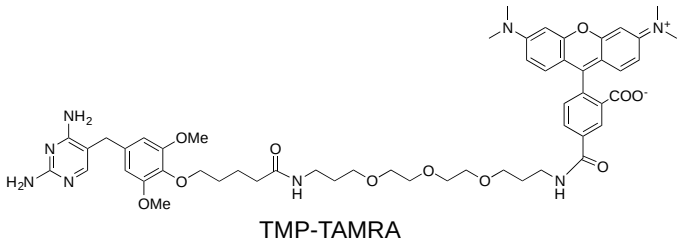

TMP-TAMRA

Figure S6: Structure of TMP-TAMRA, the fluorescent probe used for fluorescence polarization competition assays with TMP-T.

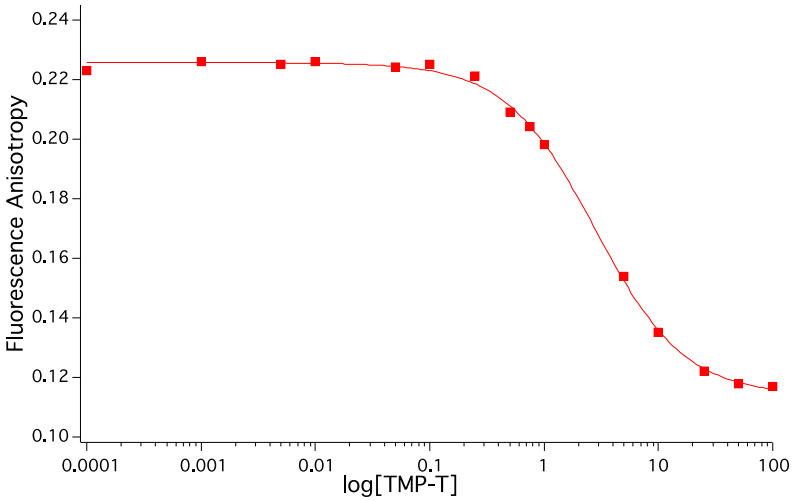

Figure S7: Semilog plot of fluorescence anisotropy as a function of TMP-T concentration. Red squares represent data points and the red line is the best fit to a sigmoidal binding curve in Igor Pro with a midpoint (IC50) of 2.8 ± 0.1.

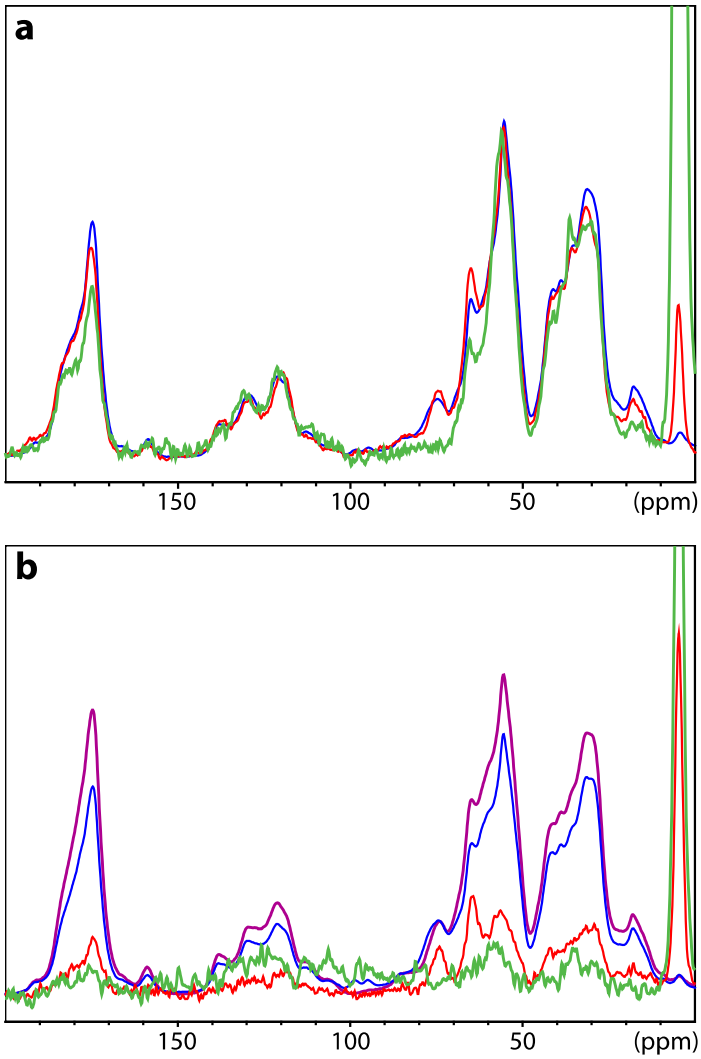

Figure S8: Comparison of signal intensity for TMP-T **(a)** and TOTAPOL **(b)** dilution series with approximately fixed protein-to-biradical ratios (1:1 for TMP-T, ~1:2 for TOTAPOL). All spectra are scaled in order to match the highest concentration sample, taking into account the number of scans and differences in receiver gain. Therefore, in the absence of concentration effects, all the spectra in each panel should exhibit identical intensities. TMP-T shows very little decline in enhancement as DHFR concentrations are lowered by almost two orders of magnitude from 4.5 mM (blue) to 0.5 mM (red) and finally to 50 μM (green), by virtue of its binding specificity to DHFR. TOTAPOL enhancements decline markedly with decreasing DHFR concentrations: 6.5 mM (purple), 5.0 mM (blue), 0.5 mM (red), and 0.05 mM (green). All spectra were acquired using CP from ^{1}H with 100 kHz SPINAL decoupling[2] during detection, an MAS frequency of 8 kHz, a temperature of 106 K and with continuous microwave irradiation. Scaling factors are as follows, in order of discussion: (a) 1.0, 9.0, 90.0 and (b) 1.0, 1.3, 13.0, 130.0.

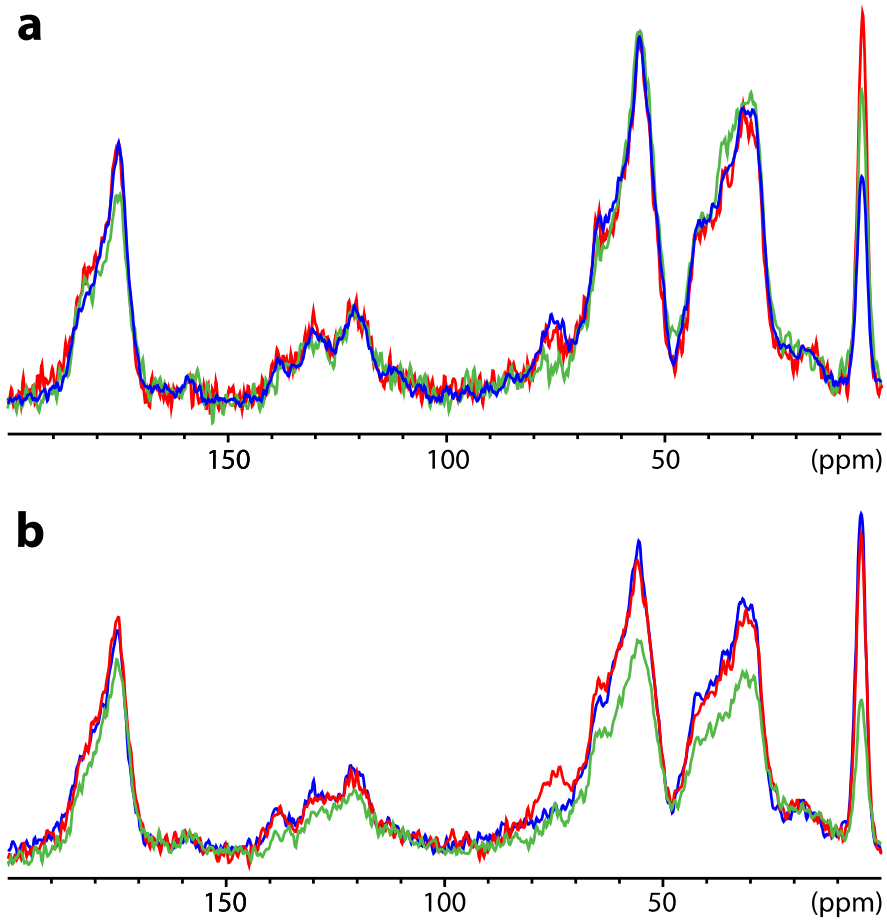

Figure S9: Overlay of **(a)** TMP-T and **(b)** TOTAPOL biradical concentration series. Virtually no bleaching is observed as TMP-T is titrated from substoichiometric (2.7 mm TMP-T, blue) to stoichiometric (4.5 mM TMP-T, red) to super stoichiometric (7.0 mM TMP-T, green), Silicone disk intensity at 4 ppm should be ignored, as it is not enhanced. For TOTAPOL, little bleaching is observed between 4 mM (blue) and 10 mM (red). However, significant paramagnetic bleaching of the aliphatic, Cα (~60 ppm), and aromatic regions is observed at 20 mM concentration (green). Due to the lower solubility of TMP-T, concentrations around 20 mM could not be achieved for direct comparison. However, such concentrations are unnecessary as superstoichiometric TMP-T already provides DNP enhancements higher than 20 mM TOTAPOL. All spectra were acquired at 600 MHz ^{1}H field using CP from ^{1}H with 100 kHz SPINAL decoupling during detection, at an MAS frequency of 8 kHz, a temperature of 105 K, and without microwave irradiation. All spectra in each panel were scaled to match the DHFR concentration of the first titration point (blue spectrum) – scaling factors are as follows: (a) 1.00, 1.09, 1.63 and (b) 1.00, 1.50, 1.15 for blue, red, and green spectra, respectively.

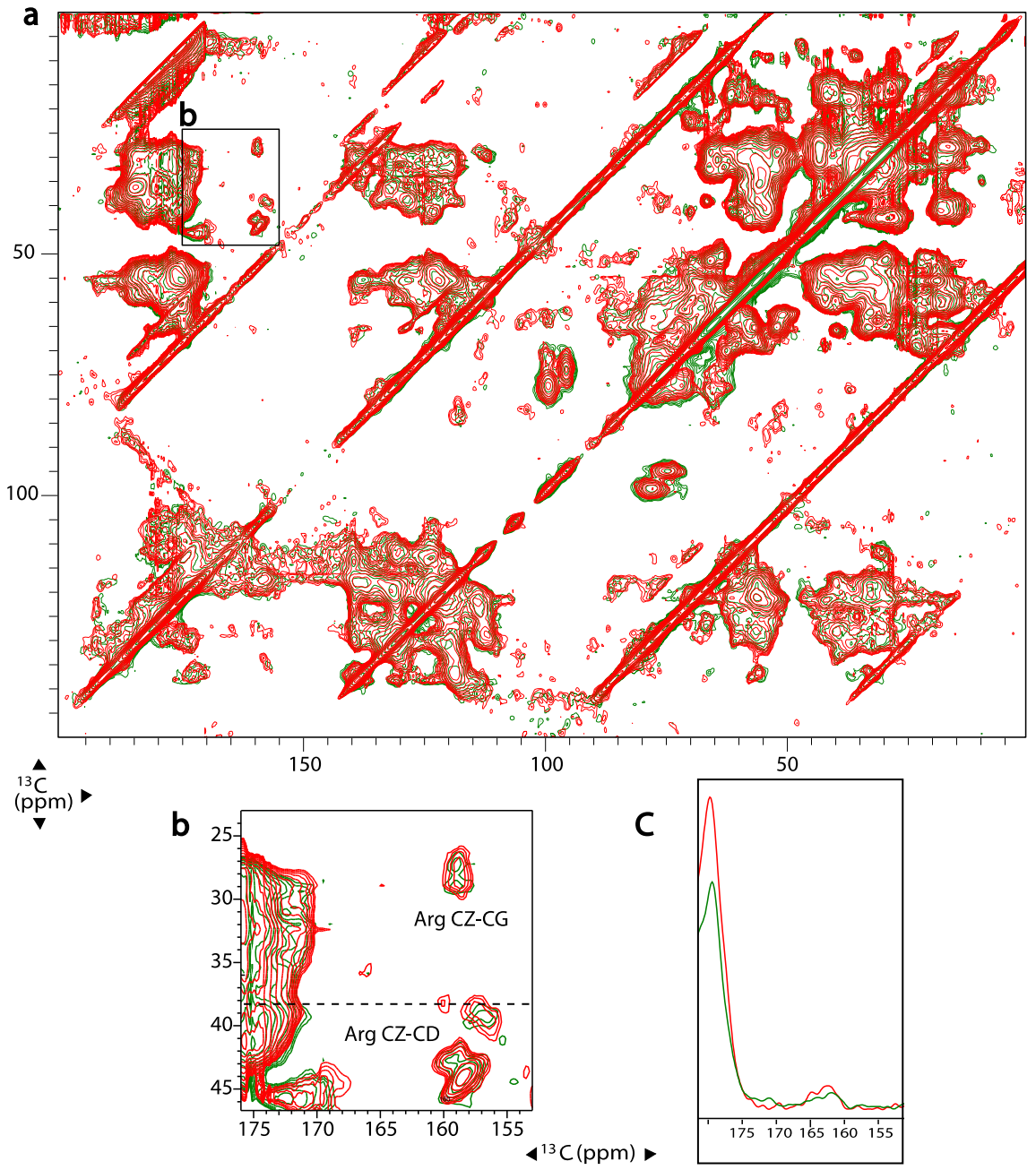

Figure S10: Overlay of 2D ^{13}C-^{13}C DARR spectrum with sample 4.5 mM 1:1 DHFR: TMP-T shown in red and 10 mM TOTAPOL, 6.5 mM DHFR in green. These spectra indicate more bleaching caused by TOTAPOL than by TMP-T. All spectra were acquired at an MAS rate of 8 kHz, at a temperature of 106 K, and with continuous microwave irradiation and were scaled to account for protein concentration.
(a) ^{13}C-^{13}C correlation spectra acquired using 20 ms of DARR mixing.[10]
(b) Close-up of (**a**) in arginine CZ region.
(c) Horizontal slice through (**b**) at frequency indicated by dashed line.

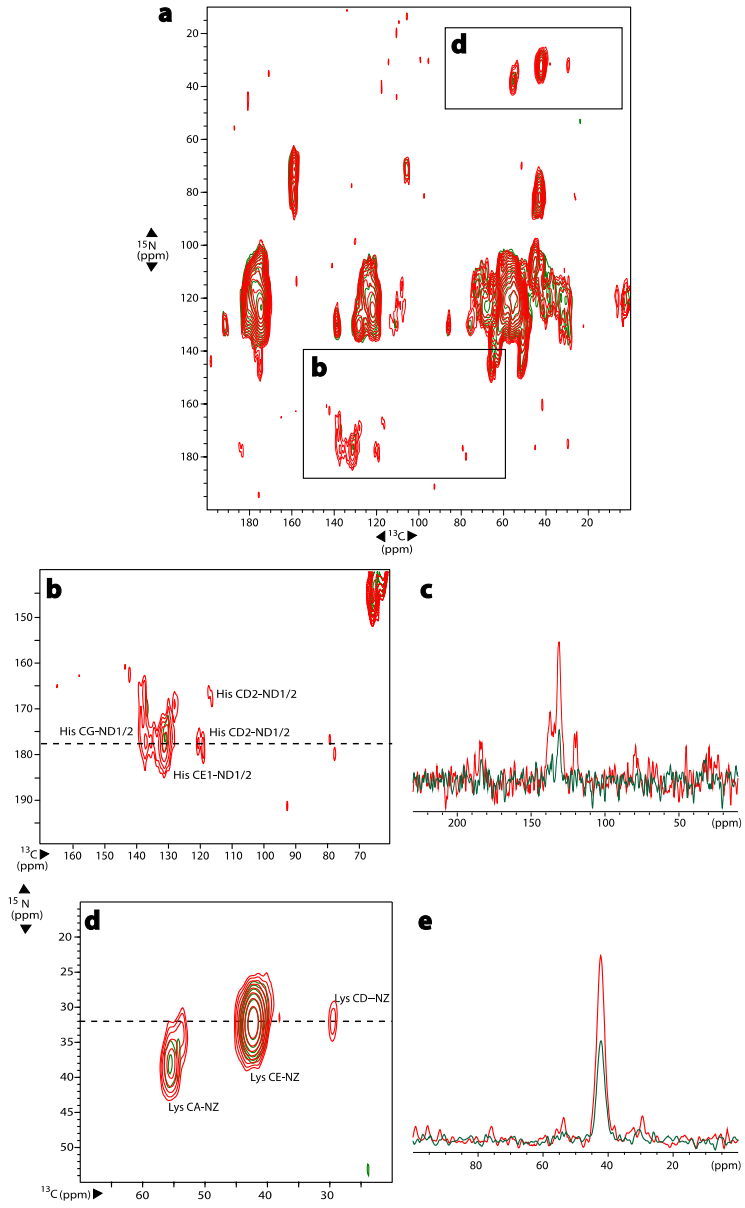

Figure S11: Overlay of 2D ^{15}N-^{13}C TEDOR spectrum with 4.5 mM 1:1 DHFR:TMP-T shown in red and 10 mM TOTAPOL, 6.5 mM DHFR in green. These spectra indicate that more bleaching is caused by TOTAPOL than by TMP-T. Spectra were acquired at 8 kHz MAS, at a temperature of 106 K, with continuous microwave irradiation, and were scaled to account for protein concentration.
(a) full z-filtered TEDOR[11] spectrum acquired with 1.5 ms of mixing time (12 rotor cycles).
(b,d) close-up of ^{15}N-^{13}C spectrum in histidine and lysine regions, respectively.
(c,e) horizontal slices through (**b**) and (**d**), respectively, at frequency indicated by dashed line.

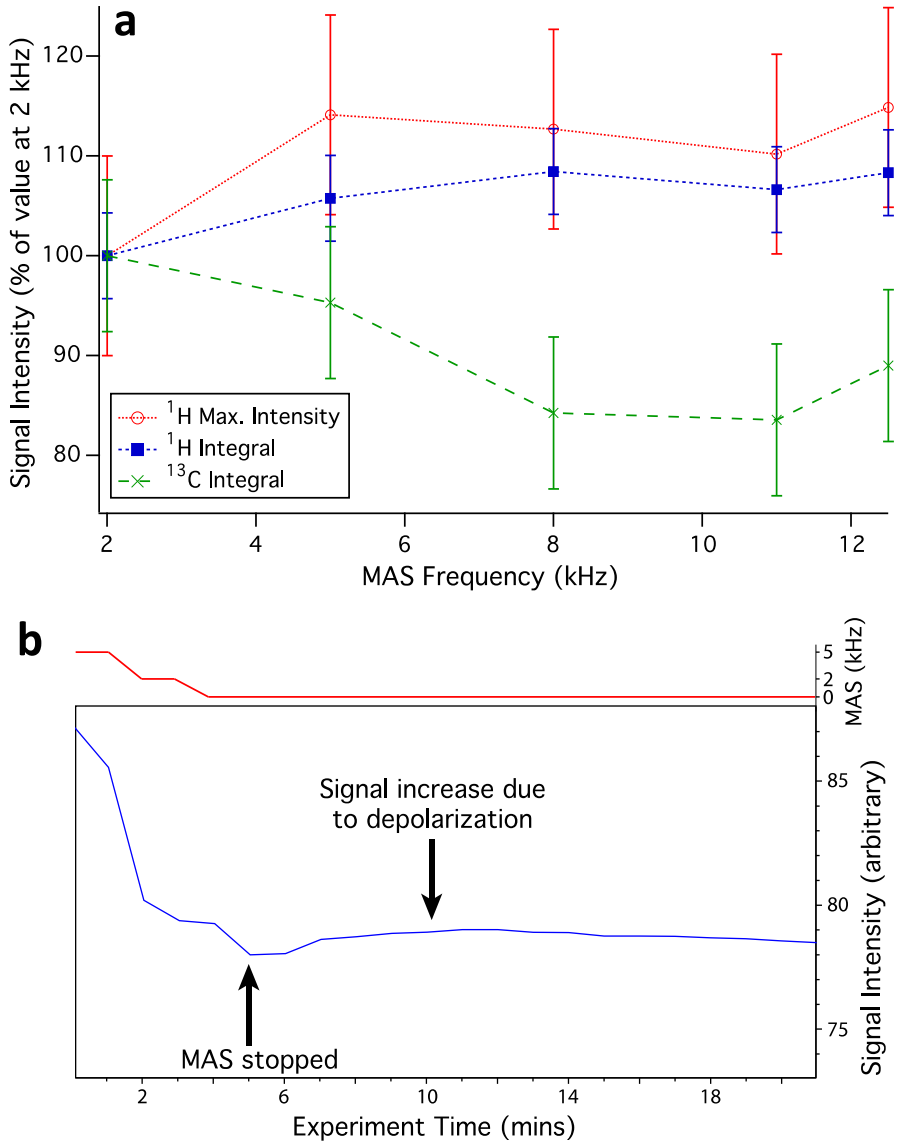

Figure S12: Characterization of the MAS dependent depolarization in 0.5 mM 1:1 DHFR/TMP-T complexes with microwaves off. **(a)** The ^{1}H and ^{13}C signal as a function of MAS frequency, normalized to the intensity at 2 kHz MAS. Signal intensity does not decrease significantly as MAS frequency increases, indicating that depolarization is not a major factor. Errors of the measurement were estimated from signal intensity/integral variation on a standard proline sample during a 24-hour stability array under the same conditions. **(b)** When MAS is stopped in an experiment to assess the level of depolarization, signal intensity does not increase significantly after MAS is stopped (unlike in Thurber and Tycko, 2014) [12], indicating that MAS dependent depolarization of the ^{1}H spins is not occurring.
Spectra were acquired at 600 MHz without microwave irradiation at a sample temperature of 106°±1ºK. ^{1}H spectra were acquired with a one pulse Bloch decay, and ^{13}C experiments via CP from ^{1}H with 100 kHz of SPINAL decoupling during detection.

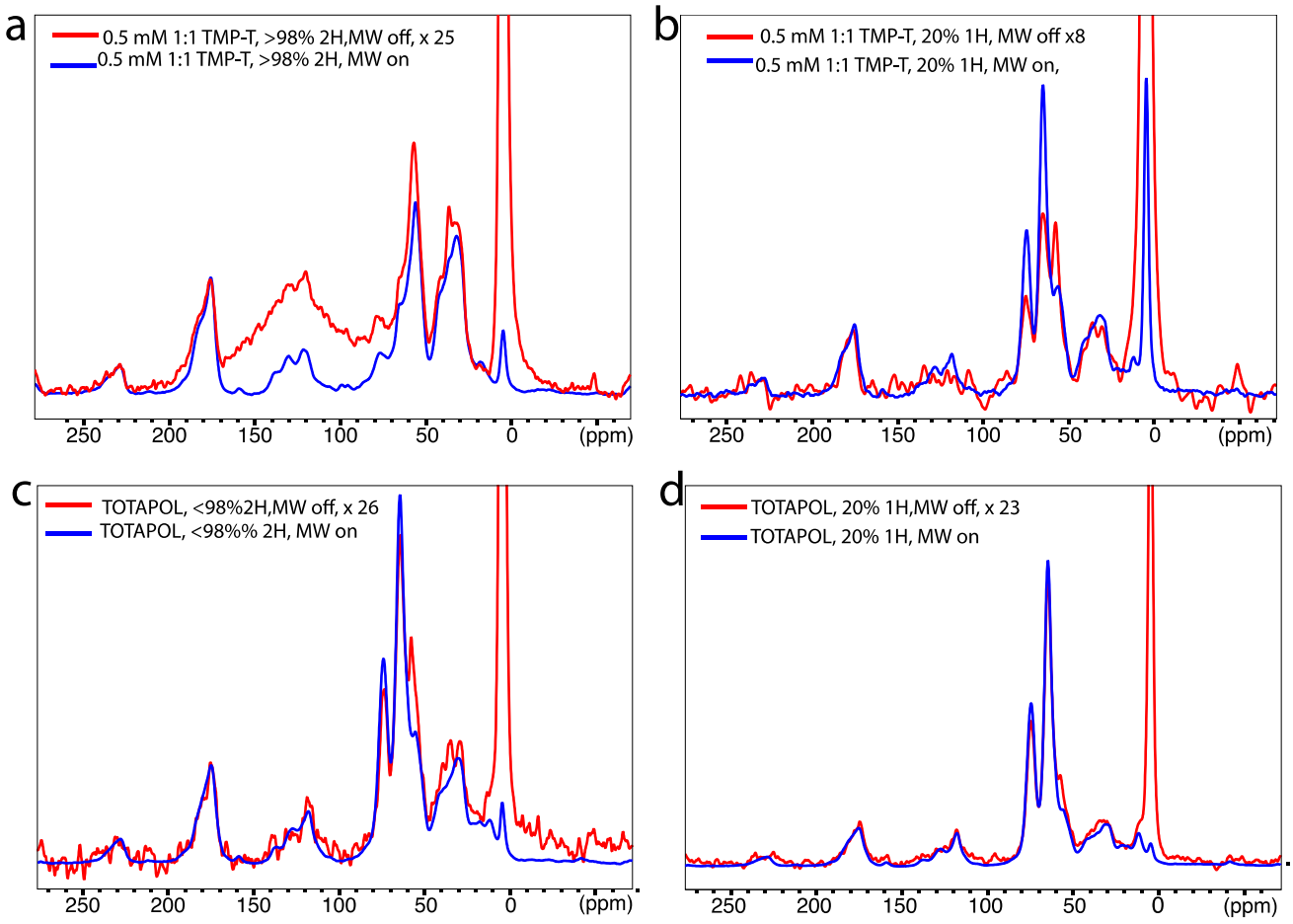

Figure S13: MW off (**red**) and MW on (**blue**) for deuterated **(a)** and protonated **(b)** 0.5 mM TMP-T 1:1 samples, respectively. In the deuterated sample, enhancement on the protein is larger than enhancement on glycerol peaks. In the protonated sample, enhancement on the protein is less than that on the glycerol. For similar samples prepared with 21 mM TOTAPOL, 0.5 mM DHFR **(c, d)**, enhancement is relatively uniform across the sample at both protonation levels. Spectra were acquired at 600 MHz ^{1}H field using CP from ^{1}H with 100kHz SPINAL decoupling during detection, 8 kHz MAS frequency, 106°±1ºK, and with continuous microwave irradiation.

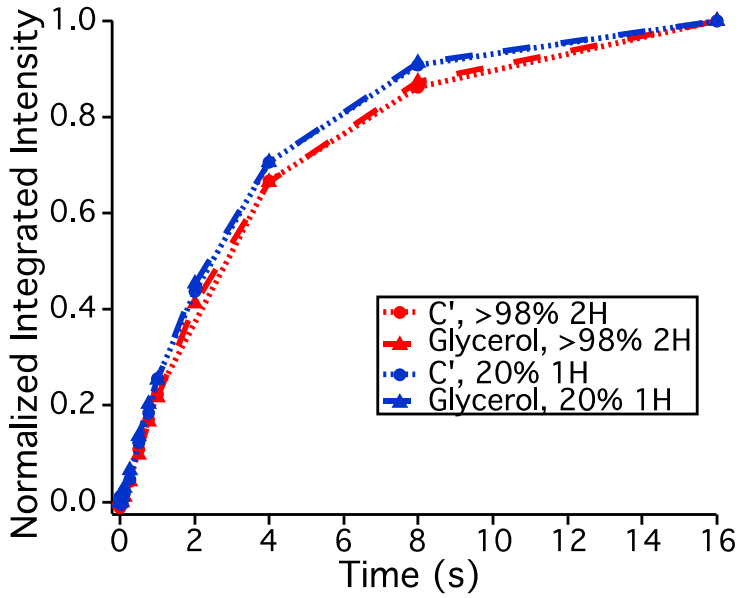

Figure S14: DNP polarization buildup curves for TOTAPOL samples at varying protonation levels show that protonation has little effect on T_B, and that the protein and glycerol have similar buildup times, in contrast to TMP-T samples (**Figure 5c**). The pulse sequence shown in **Figure S4** was used. When fit to a saturation recovery function, T_B was 4.1 s for C' and 4.2 s for glycerol at >98% ^{2}H, compared to 3.5 s for C' and 3.5 s for glycerol at 20% ^{1}H.

Supplemental References:

(1) Corzilius, B.; Andreas, L. B.; Smith, A. A.; Ni, Q. Z.; Griffin, R. G. Paramagnet Induced Signal Quenching in MAS-DNP Experiments in Frozen Homogeneous Solutions. *J. Magn. Reson.* **2014**, *240*, 113–123.

(2) Bräuniger, T.; Wormald, P.; Hodgkinson, P. Improved Proton Decoupling in NMR Spectroscopy of Crystalline Solids Using the SPINAL -64 Sequence. *Monatsh. Chem.* **2002**, *133*, 1549–1554.

(3) Hu, K.-N.; Song, C.; Yu, H.-H.; Swager, T. M.; Griffin, R. G. High-Frequency Dynamic Nuclear Polarization Using Biradicals: A Multifrequency EPR Lineshape Analysis. *J. Chem. Phys.* **2008**, *128*, 052302 1-17.

(4) Tran, V. a.; Rasmussen, K.; Grampp, G.; Kokorin, a. I. Solvent Effects on the Intramolecular Spin Exchange in Biradicals at Room Temperature. *Mol. Phys.* **2007**, *105*, 2119–2125.

(5) Parmon, V. N.; Kokorin, A. I.; Zhidomirov, G. M.; Zamaraev, K. I. On the Mechanism of Spin Exchange in Long-Chain Nitroxide Biradicals. *Mol. Phys.*

1975, *30*, 695–701.

(6) Calloway, N. T.; Choob, M.; Sanz, A.; Sheetz, M. P.; Miller, L. W.; Cornish, V. W. Optimized Fluorescent Trimethoprim Derivatives for in Vivo Protein Labeling. *Chembiochem* **2007**, *8*, 767–774.

(7) Nikolovska-Coleska, Z.; Wang, R.; Fang, X.; Pan, H.; Tomita, Y.; Li, P.; Roller, P. P.; Krajewski, K.; Saito, N. G.; Stuckey, J. A.; et al. Development and Optimization of a Binding Assay for the XIAP BIR3 Domain Using Fluorescence Polarization. *Anal. Biochem.* **2004**, *332*, 261–273.

(8) Kenakin, T. P. *A Pharmacology Primer*; Elsevier: New York, NY, 2014.

(9) Baccanari, D. P.; Daluge, S.; King, R. W. Inhibition of Dihydrofolate Reductase: Effect of Reduced Nicotinamide Adenine Dinucleotide Phosphate on the Selectivity and Affinity of Diaminobenzylpyrimidines. *Biochemistry* **1982**, *21*, 5068–5075.

(10) Igumenova, T. I.; McDermott, A. E.; Zilm, K. W.; Martin, R. W.; Paulson, E. K.; Wand, A. J. Assignments of Carbon NMR Resonances for Microcrystalline Ubiquitin. *J. Am. Chem. Soc.* **2004**, *126*, 6720–6727.

(11) Jaroniec, C. P.; Filip, C.; Griffin, R. G. 3D TEDOR NMR Experiments for the Simultaneous Measurement of Multiple Carbon-Nitrogen Distances in Uniformly 13C, 15N Labeled Solids. *J. Am. Chem. Soc.* **2002**, *124*, 10728–10742.

(12) Thurber, K. R.; Tycko, R. Perturbation of Nuclear Spin Polarizations in Solid State NMR of Nitroxide-Doped Samples by Magic-Angle Spinning without Microwaves. *J. Chem. Phys.* **2014**, *140*, 184201 1-11.

(13) Sawaya, M. R.; Kraut, J. Loop and Subdomain Movements in the Mechanism of Escherichia Coli Dihydrofolate Reductase: Crystallographic Evidence. *Biochemistry* **1997**, *36*, 586–603.

(14) Trott, O.; Olston, A. J. AutoDock Vina: Improving Speed and Accuracy of Docking with a New Scoring Function, Efficient Optimization, and Multithreading. *J. Comput. Chem.* **2010**, *31*, 455–461.